

Thermal Cyclic Fatigue Analysis of Three Aluminum Piston Alloys

P.SAI VINEETH*

*PG Scholar, Department of Mechanical Engineering, CMR Engineering college, HYDERABAD.

Abstract

The aluminum piston Al 11wt% Si alloys SC100, ACA8, A4032 were tested together with A2618-T6 concerning their mechanical properties and their thermal fatigue behavior. The alloy A2618 shows a better elongation to failure and higher yield stress compared to the other alloys by maintaining the low coefficient of thermal expansion (CTE). Thermal fatigue experiments confirmed that the Coffin-Manson equation can be used for life time prediction with the coefficients $C_p = 0.0385$, $K_p = -0.377$ comparable for A2618, while $K_p = -0.45$ for ACA8 and SC100 is obtained. The activation energy derived from the temperature dependence of life time was estimated as $Q = 0.5\text{eV}$ as typical for aluminum alloys.

Keywords: high temperature low - cycle – fatigue; plastic strain; tensile test; thermal expansion

I. INTRODUCTION

The main application as piston in engines made the Al 12wt% Si alloys famous among the groups of aluminum alloys called piston alloys [1-7]. They have high mechanical properties at elevated temperatures up to approximately 350 °C. Simultaneously, these alloys possess excellent abrasion and corrosion resistance, low coefficient of thermal expansion and high strength-to-weight ratio. Typically pistons are cast from near eutectic Al-Si alloys due to their high strength over weight ratio and good thermal conductivity and are resistant to fast temperature changes. Additions of Mn [2] or Cr and Fe [3] have improved the performance which could be explained by their microstructure [4,5].

The piston alloy development yielded in a low-Si alloy A2618 with high strength and larger elongation-to-failure. The high strength is achieved by increased amount of Fe, Cu and Mg, following the recent demand to use more and more recycling and scrap materials. Thermal cycle fatigue experiments require the measurement of stress, strain and temperature at the same time. The failure can be predicted from the accumulated plastic strain either by Manson-Coffin equation for low cycle fatigue (LCF) or by Basquin equation for high cycle fatigue (HCF) [7-10]. In wet atmosphere [11] crack propagation becomes the time determining factor and then Paris law [12] is used for life time prediction. The diffusion coefficient in Al is so high, that precipitates can grow even at room temperature [13]. The activation energy for self-diffusion is $Q = 142\text{ kJ/mol}$ [14].

The goal of this paper is to characterize the thermal fatigue behavior of the commercially available piston alloys SC100, ACA8A and A2618-

T6. After describing the tensile and thermal expansion properties, thermal fatigue was studied in order to compare the three different alloys.

II. EXPERIMENTAL DETAILS

Extruded bars with 1m length were cut into 200 mm pieces and machined into test pieces shown in fig. 1. The chemical composition of four tested alloys is shown in table 1. All alloys were used as received from the manufacturer with heat treatment T6. The microstructures of the longitudinal and transverse sections of alloy A2618 are shown in figure 2 a and b. The material has a grain size of about 10 μm and 50 μm along the extrusion direction. The chemical compositions in wt% of the tested alloys are shown in table 1 together with A4032 for comparison.

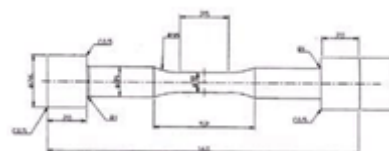
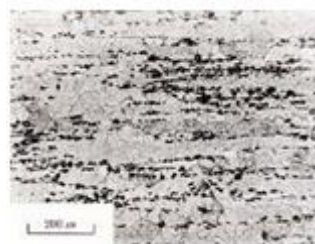


Figure 1 Length in mm of dogbone shaped specimen

(a)



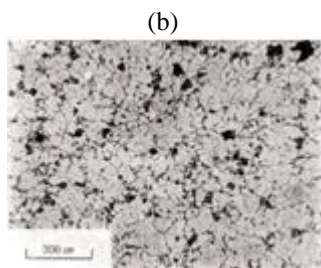


Figure 2. Optical micrograph of the A2618 specimens before deformation (a) along deformation axis (b) cross section.

Table 1 Chemical composition in wt% of the four tested alloys

Alloy	Si	Fe	Cu	Mn	Mg	Cr	Zn
A2618	0.17	1.14	1.79	0.00	1.15	0.00	0.00
SC100	10.7	0.20	3.10	0.29	0.60	0.01	0.01
A4032	11.3	0.80	0.85	0.04	1.10	0.10	0.25
ACA8A	11.9	0.16	1.01	0.01	1.11	0.00	0.00

The severpulser (EHF-ED100kN TF20L from Shimadzu, Japan) with inductive heating was used for the thermal fatigue experiments. The strain meter 6M52 was attached to the specimen and the data stored on NEC personal computer. The temperature was applied in pulsating sawtooth shape. The resulting strain and stress are simultaneously recorded during this strain controlled fatigue test.

III. RESULT AND DISCUSSION

3.1. Mechanical properties

The results of the tensile tests with strain rate $1.75 \cdot 10^{-6}$ 1/s are shown in figure 3. The alloy A2618 shows the largest elongation to fracture and largest yield stress. The Vickers hardness as function of temperature is shown in figure 4 to-

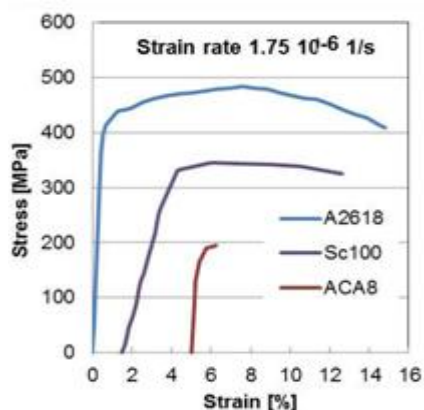


Figure 3. Stress-strain diagram obtained by tensile test experiment

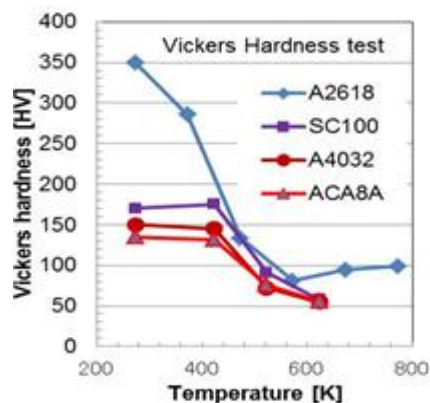


Figure 4. Vickers hardness as function of temperature for the alloys as marked

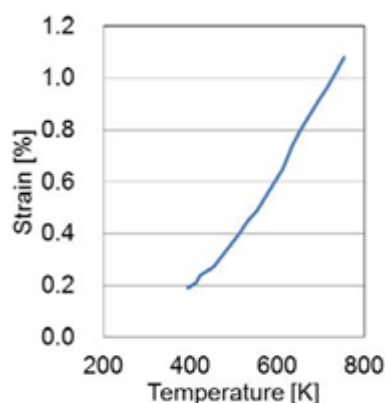


Figure 5. Strain due to thermal expansion as function of temperature for alloy A2618

gether with alloy A4032 and others for comparison. Figure 5 shows the strain obtained in heating experiment for alloy A2618. The coefficient of thermal expansion (CTE) could be estimated from the slope in fig. 5. The values for the other alloys are summarized in table 2, where elasticity modulus, yield strength, maximum strength, elongation to failure and CTE are shown. Alloy A2678 has the highest CTE= $25.9 \cdot 10^{-6}$ 1/K.

3.2. Thermal cycle properties

Thermal fatigue estimates the life time of specimens which are fixed in length, when the temperature varies from room temperature up to the maximum temperature of $T = 623$ K. The stress at thermal fatigue reaches 200 MPa at the first ten cycles, and then gradually decreases due to accumulated plastic deformation. A typical thermal cycle ($N=130$) is show in the hysteresis loop in figure 6. During the heating period the tensile stress decreases due to thermal expansion and turns into a compressive stress with negative values when reaching the maximum temperature. During cooling it gradually decreases and changes into tensile stress.

The maximum tensile stresses and compressive stresses are summarized in figure 7 as a function of cycles. The tensile stress is always larger than the compressive stress. The alloy A2618 with the larger strength builds up larger stresses compared to the alloy ACA8 with its lower strength. The alloy SC100 behaves almost like ACA8.

The plastic strain is obtained from the total strain hysteresis loop by subtracting the elastic part from the total strain.

$$\epsilon_{tr} = \epsilon_{el} + \epsilon_{pl} \quad (1)$$

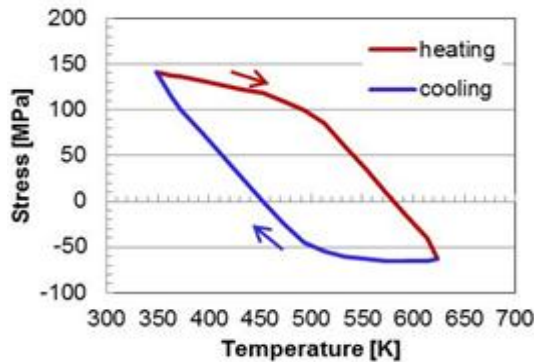


Figure 6. Stress measured during one intermediate cycle

Table 2 Mechanical properties of the four tested alloys

Alloy	E-Modul [GPa]	Yield strength [MPa]	Max. Stress [MPa]	Elong. Fail. [%]	CTE [$10^{-6} 1/K$]
A2618	73.7	420	480	15.5	25.9
SC100	78	368	413	11	21.1
A4032	79	315	380	8	19.2
ACA8A	80	310	335	1	20.7

(N=130) for alloy A2618-T6

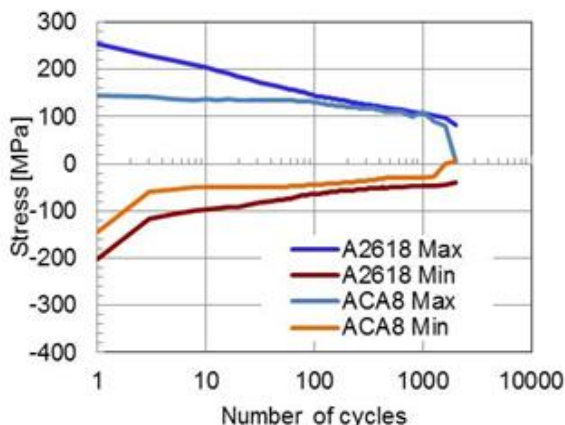


Figure 7. Stress dependence on the number of cycles for alloys A2618-T6 and ACA8

The results of the thermal cycle fatigue experiments for several temperatures are shown in figure 8. The plastic strain is large for high temperatures and low at low temperatures. The criterion for failure is the accumulated plastic strain and saturates at a level of 100MPa. The accumulated plastic strain is proportional to the maximum temperature.

Figure 8 shows the plastic strain as a function of the number of cycles for experiments on A2618 for different temperatures.

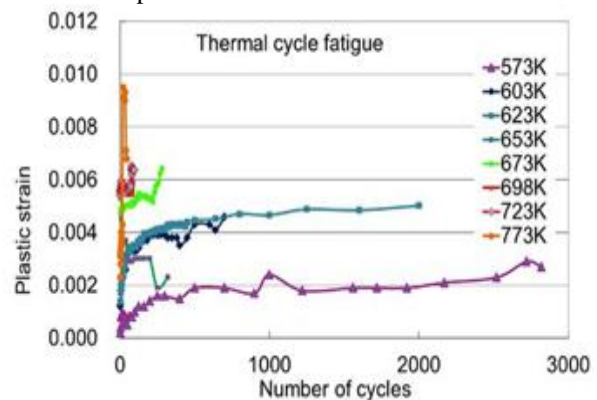


Figure 8. Plastic strain during thermal fatigue cycles for alloy

A2618-T6 at different maximum temperatures

We confirmed that the plastic strain is linear to the maximum temperature by equation (1). According to the Manson-Coffin equation the life time N_f is related to the accumulated plastic strain of each cycle:

$$\sum \epsilon_{pl} = C_p \cdot N_f^{K_p} \quad (2)$$

By plotting the life time as a function of the plastic strain, a linear behavior is observed within the error bars for all specimens. The coefficients are estimated for A2618 as $C_p = 0.0385$, $K_p = -0.377$, for ACA8 as $C_p = 0.011$, $K_p = -0.47$, and for SC100 as $C_p = 0.025$, $K_p = -0.45$. The fatigue life times for thermal fatigue for maximum temperatures below 600K are much longer for the alloy A2618-T6 compare to the two other alloys, while above 600 K the alloy ACA8 has a slightly longer life time.

Figure 9 shows the technically important diagram “number of cycles to failure” in logarithmic scale as a function of the maximum temperature at thermal fatigue. By fitting the data for A2618 by an Arrhenius plot

$$N_f = A \exp(Q_1 / kT) \quad (3)$$

with k Boltzmann constant and T temperature, we obtain $A = 0.06$ and an activation energy $Q_1 = 8 \cdot 10^{-20} J = 800 kJ/mol = 0.5 eV$. This energy corresponds to about one third of the bonding energy as obtained by the self-diffusion coefficient (140 kJ/mol), and is

typical for material damage by fatigue or creep [14]. As thermal fatigue data are very rare in literature, we plan to do such analysis in future on other materials.

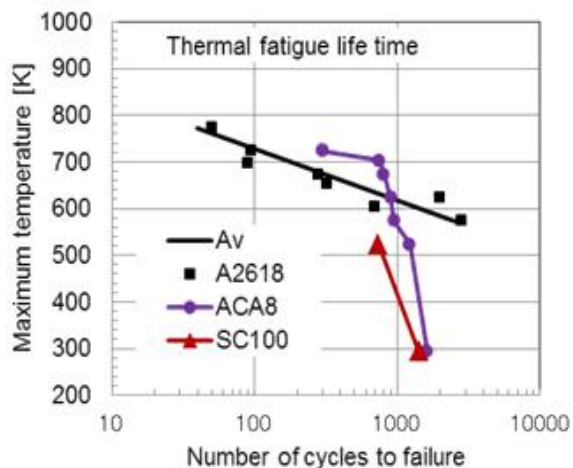


Figure 9. Life time in thermal fatigue as a function of maximum temperature for three piston alloys

IV. CONCLUSIONS

In this research, thermo-cycle fatigue tests were performed on aluminum piston alloys ACA8, SC100 and A2618-T6 at elevated temperatures up to 673 K under ambient atmosphere. The obtained results are as following.

1. The elongation to failure, hardness, and the yield strength of A2618-T6 is better than the two other alloys.
2. The stress at thermal fatigue at $T = 623\text{K}$ reaches 200 MPa at the first ten cycles and saturates at a level of 100MPa. The accumulated plastic strain is proportional to the maximum temperature.
3. Alloy A2618-T6 has much longer thermal fatigue life times for maximum temperatures below 600K as compared to the two other alloys, only above 600 K the alloy ACA8 has a slightly longer life time, but the failure occurs suddenly.
4. The fatigue life can be predicted by the Manson-Coffin rule with the parameters $C_p = 0.0385$, $K_p = -0.377$ for the A2618 alloy. The value of the activation energy for damage is 0.5 eV and is in good agreement to other aluminum alloys.

V. ACKNOWLEDGMENT

The authors acknowledge help to Shinichi Taguchi for obtaining part of the experimental data.

REFERENCES

[1] M.M. Haque, M.A. Maleque Effect of process variables on structure and properties of aluminum-silicon piston alloy, *Journal of Materials Processing Technology* 77 (1998) 122-128.
[2] Z. Qian, X. Liu, D. Zhao, G. Zhang, Effects of

trace Mn addition on the elevated temperature tensile strength and microstructure of a low-iron Al-Si piston alloy, *Materials Letters* 62 (2008) 2146-2149.
[3] Y. Li, Y. Yang, Y. Wu, Z. Wei, X. Liu, Supportive strengthening role of Cr-rich phase on Al-Si multicomponent piston alloy at elevated temperature, *Mat. Sci. Eng. A* 528 (2011) 4427-4430.
[4] M.Zeren The effect heat-treatment on aluminum-based piston alloys. *Mat. Design* 28 (2007) 2511-2517.
[5] R.X Li, R.D Li, Y.H Zhao, L.Z He, C.X Li, H.R Guan, Z.Q Hu, Age-hardening behavior of cast Al-Si base alloy. *Mat. Let.* 2004;58:2096-2101.
[6] G.H. Zhang, J.X. Zhang, B. Chao, L.W. Cai, Characterization of tensile fracture in heavily alloyed Al-Si piston alloy, *Prog. Natural Science Mat.Int.* 21 (2011) 380-385
[7] N. Eswara Prasad, D. Vogt, T. Bidlingmaier, A. Wanner, E. Arzt, High temperature, low cycle fatigue behavior of an aluminum alloy (Al-12Si-CuMgNi) *Mat. Sci. Eng. A* 276 (2000) 283-287.
[8] G. Eisenmeier, B. Holzwarth, H.W. Hoepfel, H. Mughrabi, Cyclic deformation and fatigue behavior of the magnesium alloy AZ91, *Mat. Sci. Eng. A* 319-321 (2001) 578-582.
[9] M.S. Song, Y.Y. Kong, M.W. Ran, Y.C. She, Cyclic stress-strain behavior and low cycle fatigue life of cast A356 alloys, *Int. Jour. Fatigue* 33 (2011) 1600-1607.
[10] Hayato Mouri, Wilfried Wunderlich, Morihito Hayashi, New aspects about reduced LCF-life time of spherical ductile cast iron due to Dynamic Strain Aging at intermediate temperatures, *J Nucl. Mat.* 389 [1] (2009) 137-141.
[11] W. Wunderlich, A. Niegel, H.J. Gudladt, TEM-Studies of Grain Boundaries in Cyclically Deformed Al-Zn-Mg- Bicrystals, *Acta Metall. Mater.* Vol.40 Nr.9 (1992) 2123-2129, doi:10.1016/0956-7151(92)90129-3.
[12] M. De-Feng, H. Guo-Qiu, H. Zheng-Fei, L. Xiao-Shan, Z. Wei-Hua, Effect of microstructural features on fatigue behavior in A319-T6 aluminum alloy, *Mat. Sci. Eng. A* 527 (2010) 3420-3426.
[13] J. Lendvai, W. Wunderlich, H.-J. Gudladt, Formation of L12 ordered Precipitates At Room Temperature and Their Effect on the mechanical Properties in Al-Li-Alloys, *Phil. Mag. A* 67 (1993) 99-107.
[14] O.D. Sherby, E.M. Taleff, Influence of grain size, solute atoms and second-phase particles on creep behavior of polycrystalline solids, *Mat. Sci. Eng. A* 322 (2002) 89-99.